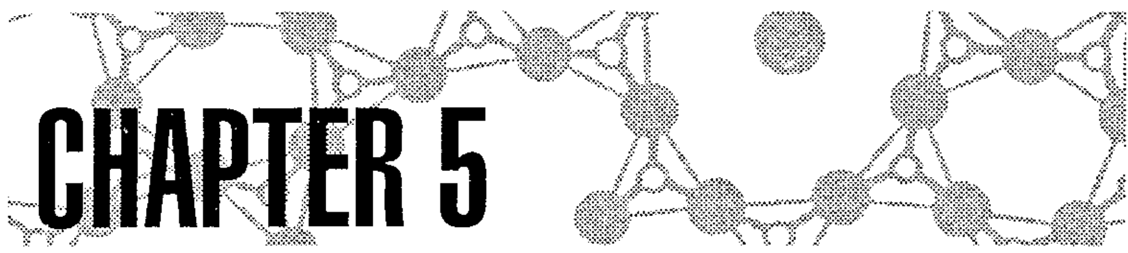

X-RAY PHOTOELECTRON SPECTROSCOPY OF GLASS

Carlo G. Pantano
Department of Materials Science and Engineering
The Pennsylvania State University
University Park, PA 16802 USA

ABSTRACT

The fundamental basis of x-ray photoelectron spectroscopy (XPS) is presented with an emphasis on those aspects of the method that are important in the analysis of glasses. The capabilities of the technique for characterizing specific features of the chemical structure and surface chemistry of glass are reviewed. The issues associated with the compositional analysis of glass surfaces are discussed in some detail. Finally, examples of the use of XPS in glass science are presented; these include: the study of (i) non-bridging oxygen in glass, (ii) hydrogen surface treatments of lead-silicate glass, (iii) nitridation of silica sol/gel thin-films, and (iv) organic adsorbates on glass fibers.

INTRODUCTION

X-ray photoelectron spectroscopy (XPS) is an analytical technique that is widely used for chemical characterization of solids. Figure 1 illustrates a typical arrangement for XPS. The specimen is irradiated with monochromatic x-rays to cause the emission of photoelectrons and Auger electrons. The energy distribution of the ejected electrons is measured to obtain the photoelectron spectrum. An example is presented in Figure 2. Each of the peaks represent the photoelectrons or Auger electrons ejected from elements in the specimen surface. The energies of the various peaks are used to identify the elements present in the sample surface, while their relative intensity provides information about the composition. Often, the *energy* values of the electrons are slightly different in a compound or multicomponent material relative to their elemental state. These small *chemical shifts* are indicative of local chemical environment, bonding, or oxidation state of the specific elements detected.

In general, XPS provides information about the elemental composition and their chemical state. It is best known for its ability to provide surface analyses because the ejected electrons originate within the outermost few atomic layers of the

To the extent authorized under the laws of the United States of America, all copyright interests in this publication are the property of The American Ceramic Society. Any duplication, reproduction, or republication of this publication or any part thereof, without the express written consent of The American Ceramic Society or fee paid to the Copyright Clearance Center, is prohibited.

specimen surface. Nevertheless, it is also possible to obtain information about the bulk.

ESCA, *electron spectroscopy for chemical analysis*, is a more general term which is often used synonymously with XPS. It emphasizes the chemical aspects of the technique, and does not exclude analysis of the Auger electrons that are always present in the photoelectron spectrum. In fact, the combined analysis of the Auger electrons, and the photoelectrons, can be most advantageous in the evaluation of insulators.

It is, of course, possible to generate photoelectron spectra with any photon excitation of the specimen. The x-ray irradiation used in XPS enhances sensitivity to the core-level electronic states, and thereby, to the atomic composition of the material. The related method of ultraviolet photoelectron spectroscopy (UPS) is based upon ultraviolet irradiation of the specimen. This enhances sensitivity to the valence-band electronic structure of the materials. Most recently, the use of synchrotron light sources has further expanded the capabilities of photoelectron spectroscopy for probing electronic structure and bonding configuration. To date, these methods have been applied to only a limited extent in glass research [1].

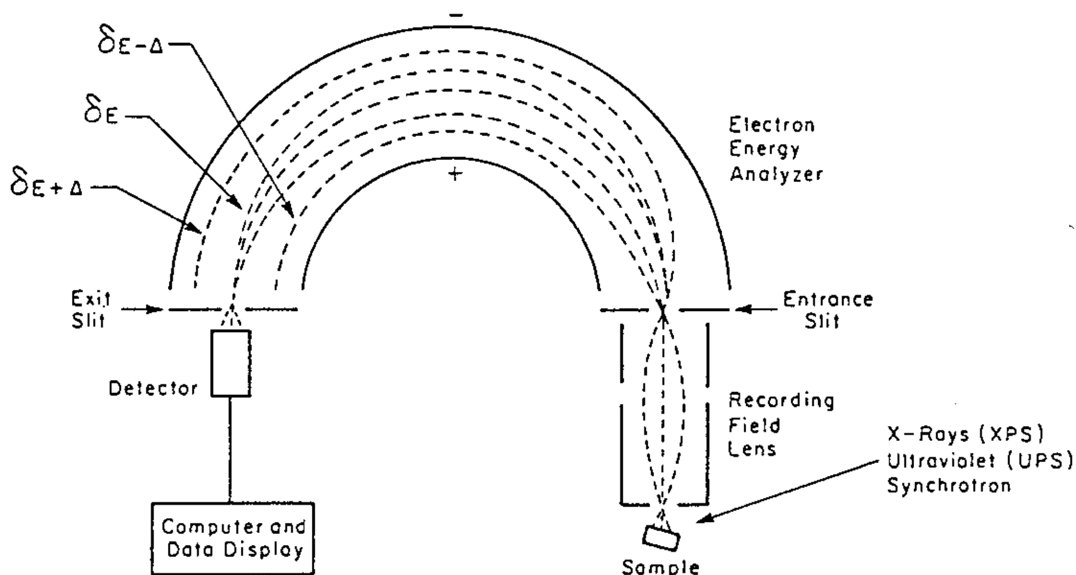

Figure 1. Schematic representation of the typical experimental arrangement for XPS; all components are contained in vacuum.

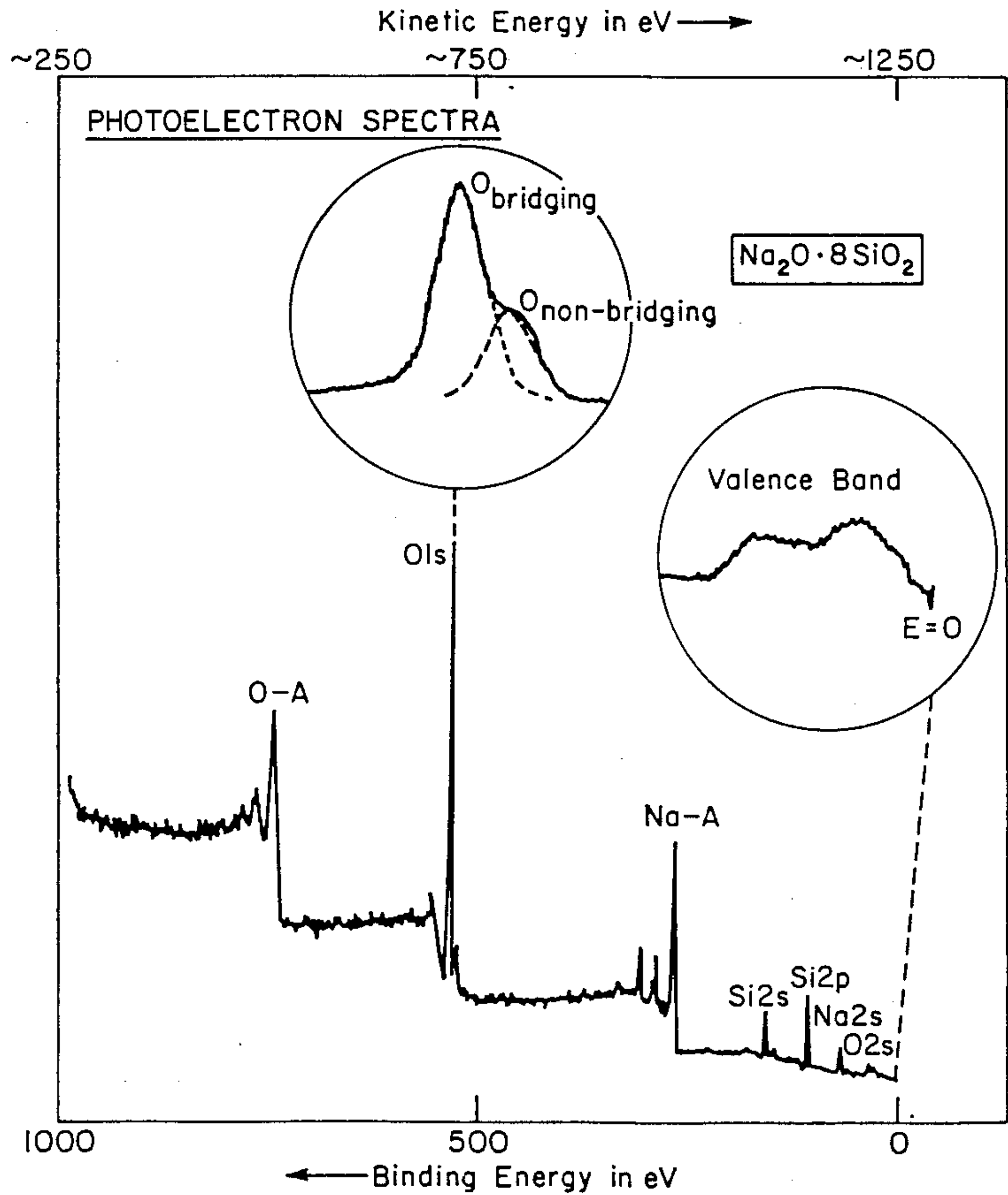

Figure 2. A typical XPS spectrum for the vacuum fracture surface of a glass; the insets are high resolution spectra of the Ols and valance band regions.

XPS can be applied in many different ways to study or analyze glass [2]. The most important and routine applications of XPS in glass research include analysis of the surface composition, surface chemical state, or bulk chemical structure. More specifically,

- elemental surface composition,
- organics on surfaces,
- non-bridging oxygen concentration in the bulk,
- oxidation state of cations on the surface or in the bulk,
- valence band density of states.

The purpose of this chapter is to describe only the basic aspects of XPS. The important issues in spectral interpretation will be explained using specific examples in glass research. The interested reader can find more detailed discussions of photoemission theory, instrumentation and technique in the BIBLIOGRAPHY.

There are a few general characteristics of XPS that are probably best presented here at the beginning. First, XPS *cannot detect hydrogen*; in some cases, indirect information about hydrogen can be inferred through chemical shifts, but not routinely. This is an intrinsic limitation of photoelectron spectroscopy that greatly influences the study of glass where hydrogen, hydroxyls and water are often present. Second, the method is intrinsically sensitive to the outermost .5-5 nm of the glass surface; hence, *XPS is a surface analytical technique*. But if a glass specimen is fractured in ultra-high vacuum, the composition of the fracture surface can be equal to the bulk composition, and in many instances, the non-bridging oxygen content and oxidation state of this surface may be equivalent to the bulk. It is in this sense that XPS is used to analyze the bulk characteristics of glasses. Third, any spectroscopic technique that relies upon the detection of charged particles is susceptible to *charging problems* when applied to insulators. Although XPS is less prone to charging problems than other electron or ion spectroscopies, problems do exist. It is important to understand the origin and nature of the charging in XPS because it can influence the results.

PHOTOELECTRON EMISSION

The orbital model of the atom in Figure 3 illustrates the fundamental basis of XPS. The absorption of an incident photon (x-ray or ultraviolet) causes the ejection of a photoelectron. The kinetic energy of the photoelectron, KE, is simply

$$KE = h\upsilon - BE \qquad (1)$$

where $h\upsilon$ is the energy of the incident photon and BE is the binding energy of the emitted electron in the atom. The binding energy of an electron is characteristic of the specific atom, and in this way, photoelectron spectroscopy provides elemental identification. And since any occupied electron state in the atom can be ejected, the entire spectrum of photoelectrons is a representation of the electronic density of states.

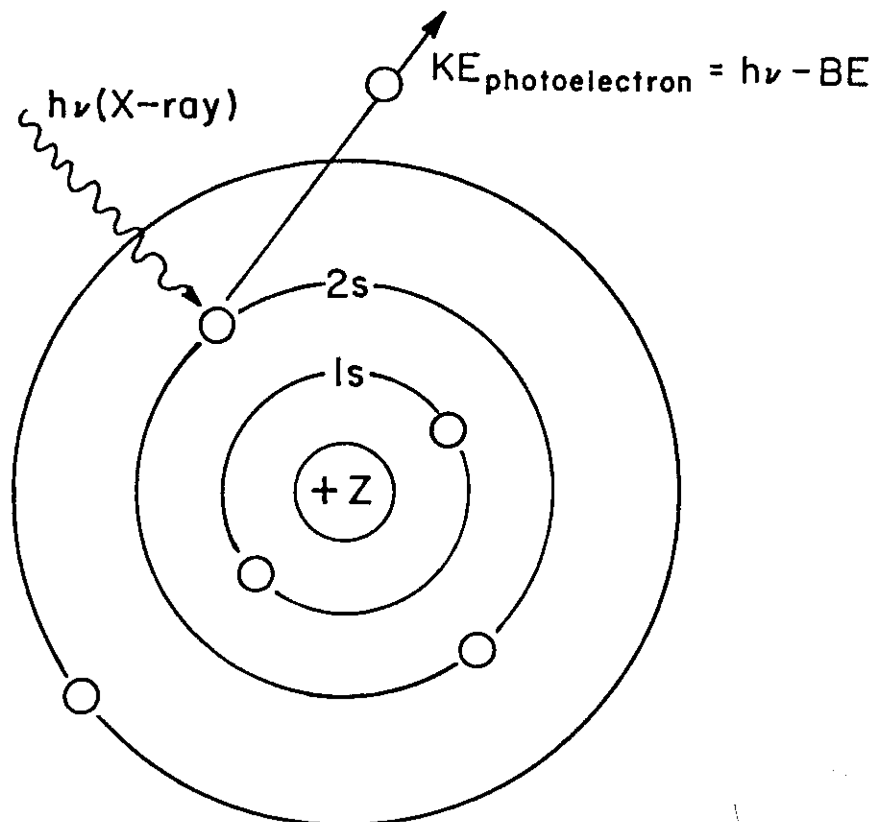

Figure 3. Orbital model of the x-ray photoemission process.

The photoelectrons distinguish the occupied electronic states only on the basis of energy. There are states corresponding to each of the principal quantum numbers 1s, 2s, 3s, ... In the case of the p, d and f levels, Russell-Saunders coupling creates two distinguishable energy states in each principal shell $2p^{1/2}$, $2p^{3/2}$, $3p^{1/2}$, $3p^{3/2}$, ... , $3d^{3/2}$, $3d^{5/2}$, $4d^{3/2}$, $4d^{5/2}$, ... , and $4f^{5.2}$, $4f^{7/2}$, $5f^{5/2}$, $5f^{7./2}$, ... There are selection rules and cross-sections that define the relative probability of photoemission in each state. And of course, photoemission cannot occur unless hυ is greater than the binding energy of the electron (typically, AlKα @ 1487 eV or MgKα @ 1254 eV are used in XPS). In general, therefore, the x-ray photoelectron spectrum is dominated by the electrons that occupy the outermost levels of the atom, e.g., the 1s electron in the case of oxygen, the 2p electrons in the case of Si, the 4f electrons in the case of Pb, etc.

The photoemission process is, in reality, more complex than equation (1) would suggest. The binding energy calculated according to equation 1 assumes the frozen orbital model (Koopman's theorem). In reality, there is some relaxation of the electrons during the photoemission process; i.e.,

$$KE = h\upsilon - BE - E_{Relaxation} \tag{2}$$

This is not an issue in routine compositional analyses because it can be accounted for through referencing and calibration. On the other hand, it can be of concern in the characterization of chemical and electronic structure.

In the case of solids, and especially insulators, the referencing of photoelectron binding energy is more complicated than the free atom models represented in eqns. 1 and 2. Figure 4 shows the energy level diagram for an atom in the solid state. The photoemission process, itself, is not affected by the solid state. But it is more sensible and practical to reference the binding energy to the Fermi level (rather than to the vacuum level). Using this reference scheme, the kinetic energy of the ejected photoelectron is reduced by the work function of the specimen, ϕ_s. Thus,

$$KE = h\upsilon - BE_f - \phi_s \tag{3}$$

The kinetic energy of the photoelectron is perturbed again upon crossing the surface barrier, ϕ_a, of the analyzer/detector. If the specimen and the analyzer/detector are in electrical contact, this perturbation is the contact potential between the specimen and the analyzer/detector (ϕ_s-ϕ_a); thus,

$$KE' = h\upsilon - BE_f - \phi_a \tag{4}$$

In the routine application of XPS, the complications suggested in equations (2), (3) and (4) are eliminated through calibration. That is, standards have been used to establish tables of self-consistent binding energies and/or kinetic energies [see B6]; essentially,

$$E_{kinetic} = h\upsilon - E_{binding}. \tag{5}$$

The assumptions are simply that the Fermi levels of the specimen surface and the analyzer/detector are equilibrated, the relaxation energy (E_R) is a constant for an element (independent of of the material composition or chemical structure), and that the analyzer/detector work function, ϕ_a, is constant. In practice, the situation is further simplified because there is always one peak in the spectrum (usually carbon) that can be used to calibrate the binding energy scale. In fact, calibration of the measured spectrum using the C1s is an almost universal practice. Here, it is assumed that so-called adventitious carbon (essentially carbonaceous surface contamination found on virtually any specimen that has been exposed to the ambient atmosphere) is either hydrocarbon or amorphous carbon, and therefore, is assigned a binding energy of 285 eV [3-4]. Of course, these assumptions must be

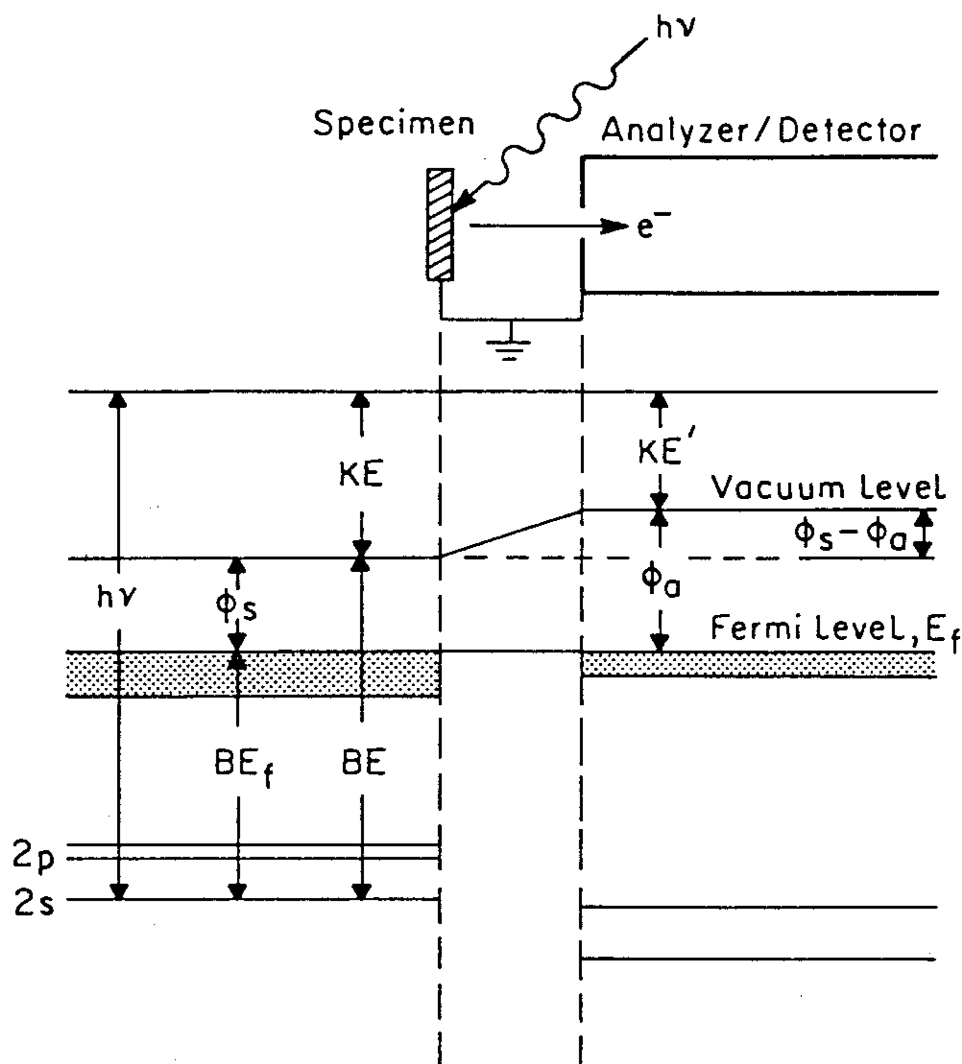

Figure 4. Energy-level references for XPS when the Fermi levels of the specimen and the analyzer/detector are equilibrated.

reconsidered in those cases where quantitative interpretation of a binding energy, or a small binding energy shift, is of interest. This is especially true in the analysis of insulators.

In the case of insulators, the specimen can *charge* due to the ejection of photoelectrons, Auger electrons, and low energy secondary electrons. This positive charging of the surface must be stabilized to obtain a useful XPS spectrum. This is usually achieved through the use of a low energy electron flood gun, although other methods have been proposed (see Appendix 2 in B5). But even if the surface potential is stable, the Fermi levels of the analyzer/detector and specimen may not be in equilibrium. Thus,

$$E_k = h\upsilon - E_b \pm E_{charge}. \qquad (6)$$

This surface potential influences all of the electrons uniformly, and so in routine analyses, the measured spectrum can be recalibrated using the carbon 1s line.

In those studies where chemical state identification is of specific interest, referencing to carbon may not be an acceptable approach. Here, it is necessary to define a more reliable reference. One method is to choose a line associated with a specie in the glass structure; essentially, an internal reference. The assumption is that the binding energy of this reference specie is independent of the composition or chemical states of the other constituents of the glass (e.g., Si 2p in many silicate glasses). Unfortunately, this is not always possible because of the collective effect of bonding and network structure upon the electron binding energies of all the atoms. Alternatively, one can implant an internal reference; for example, N_2 molecules can be implanted at very low energy (<500 eV). In this way, the N1s binding energy in N_2 can be used for calibration. The shortcoming of this approach is the possible introduction of ion beam damage, and the need for an in-situ source of low energy ions in the XPS system. It does not provide an absolute measure of the binding energy, but it does provide a reliable determination of binding energy shifts. Still another approach is to deposit a small metallic dot (usually Au) on the glass surface, and use it to pin the Fermi level of the spectrometer to the glass surface. The Au dot is grounded to the spectrometer, and the Au line that appears in the spectrum of the glass is used for calibration. This method is widely employed in research studies where precise determination of binding energy values are required; it is not routine, and is subject to careful interpretation [5-9]. In general, one must recognize real limitations in precise determinations of binding energy or chemical shifts in the case of insulating glasses.

AUGER EMISSION

After an electron vacancy is created due to the photoemission process (see Figure 3), a de-excitation process occurs within the atom to fill the vacancy. The de-excitation can occur *either* through an x-ray emission *or* through an Auger electron emission. The relative probability of these two processes depends upon the incident x-ray energy and the atomic number of the atom. During the typical XPS analysis (where soft x-rays are used), Auger emissions are prevalent – especially in

low z elements – and these electrons are necessarily included in the photoelectron spectrum.

Auger electron emission – shown schematically in Figure 5 – corresponds to the decay of an outer electron (e.g., an L-shell electron) to fill the electron vacancy (e.g., a K-shell vacancy) and then transfer of the energy difference (E_K-E_L) to another electron (e.g., another L-shell electron); hence, the nomenclature KLL Auger electron. If, alternatively, an L-shell electron was vacated due to the photoemission, an LMM Auger electron could be created. The kinetic energy of the Auger electron is characteristic of the atom; i.e.,

$$E_{KLL} = E_K - E_{L1} - E_{L2} - \phi_a \tag{7}$$

There are tables of Auger electron energies for all the elements in the periodic table, and these can be used in routine chemical analyses [see B6].

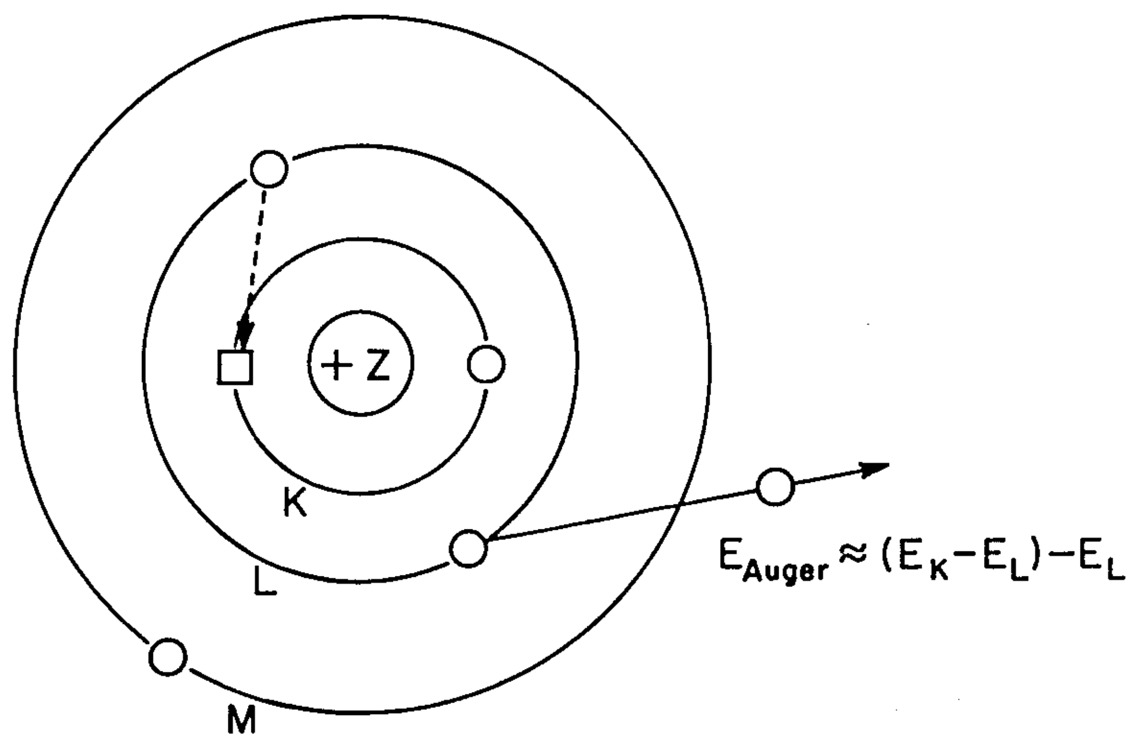

Figure 5. Orbital model of the electron transitions associated with de-excitation of a core-level vacancy (KLL) by the Auger emission process.

It is important to note that is is the *measured kinetic energy* of Auger electrons that is characteristic of the atom where it originates, while in the case of the photoelectrons, it is the *calculated binding energy* that is characteristic; i.e., the measured kinetic energy of any Auger electron is independent of the x-ray used in the analysis ($h\upsilon$), while in the case of photoelectrons, the measured kinetic energy depends upon $h\upsilon$. Thus, one way to distinguish between the Auger electron and photoelectron lines in the spectrum is to change the x-ray source. The photoelectron lines will change in kinetic energy while the Auger electron lines will always appear at their characteristic kinetic energy. In practice, though, experience and the width of the line are more often used in the proper assignment of Auger lines; Auger lines are often broader in energy than photoelectron lines.

One of the most interesting uses of the Auger lines that appear in the XPS spectrum is in the definition of *Auger parameter*. The Auger parameter, α, is the difference in kinetic energy between any Auger line and any photoelectron line for a specific element; i.e.,

$$\alpha = KE_{Auger} - KE_{Photoelectron} \tag{8}$$

This definition of Auger parameter is shown schematically in Figure 6. Ideally, the lines chosen would be directly related through a specific transition (e.g., Si 1s and Si KLL), but this is not required. In practice, it is calculated using the most intense lines in the spectrum . The Auger parameters are found to be unique to a specific compound, and in fact, have been tabulated for a wide range of substances including silicates and aluminosilicates. They are especially useful in the case of insulators because the value of α is insensitive to charging and referencing. Table 1 shows, for example, a compilation of data for silicon compounds.

CHEMICAL AND STRUCTURAL EFFECTS

The binding energy of an electron depends not only on the atomic number, but also upon the electronic structure of the atom and its surroundings. Thus, it is sensitive to the chemical bonding or structure, the oxidation state and the local chemical environment of the atom. In practice, this effect is termed a *chemical shift*; that is, a shift in the binding energy relative to the elemental state. Table 1 shows the Si2p binding energy in various Si compounds. The chemical shift is of the order of a fraction to a few eV. Thus, it is necessary to measure the photoelectron spectra at high resolution in order to extract chemical information. In general, the ability to distinguish chemical states is not apparent in a survey scan of the type shown in Figure 1. The inset in Figure 1 shows the high resolution scan for O1s. Note the presence of two peaks at this binding energy. This implies the presence of two chemical forms or states of oxygen. In this case, the bridging and non-bridging oxygens in this glass are represented.

Table 1. Peak Positions and Auger Parameters (α_{Si}) for a Variety of Si Compounds [from 10].

Sample	Formula	Si 2p BE (eV)	Si KLL KE (eV)	α_{Si} (eV)
silicon	Si	99.6	1616.4	462.4
silicon carbide	SiC	103.9	1610.2	460.5
silicon nitride	Si_3N_4	102.0	1611.7	460.1
silicon dioxide	SiO_2	102.6	1609.6	458.6
zinc silicate	$ZnSiO_3$	108.1	1603.7	458.2
silica gel	$SiO_2{\cdot}xH_2O$	107.0	1604.3	457.7

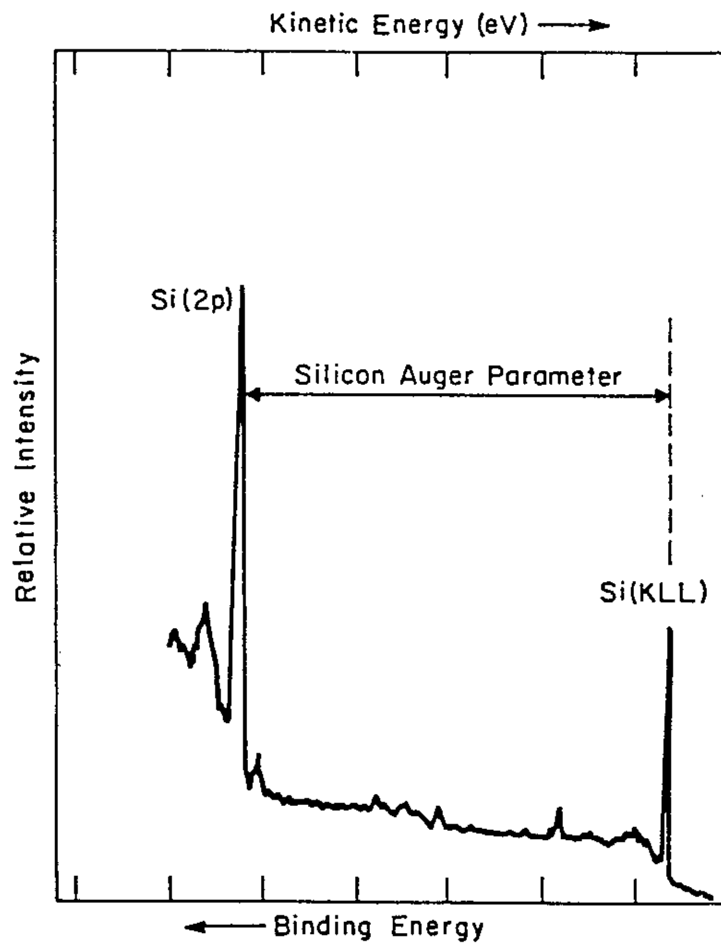

Figure 6. Spectral description of the Auger parameter (α) for Si; in this case, the Si(KLL) transition was excited with bremsstrahlung radiation.

Many theories and approaches have been developed to understand and interpret binding energy shifts. The simplest and most basic idea can be realized using the charged shell model. It assumes that increases or decreases in the electron charge density in the outer bonding orbitals causes complementary changes in the binding energy of the inner core levels. Thus, the Si 2p binding energy is higher in SiC, Si_3N_4 or SiO_2, than in Si due to the electronegativity of the bonding environment; i.e., the electron charge density near the Si atom is decreased, and thereby the Si 2p core level electron is more tightly bound. Similarly, the binding energy of the O 1s in a non-bridging site (NBO) is less than in a bridging site because the higher charge density at the NBO shields the inner-level 1s electron and thereby lowers its effective binding energy. This simple, qualitative concept is useful for understanding the origin and sign of the shift. But the magnitude of the shift depends upon many factors including relative electronegativity of the bonded species, coordination number, relaxation effects, etc. In the case of the silicon compounds, SiC, Si_3N_4, and SiO_2, wherein the coordination number is always four, the Si 2p shift scales directly with the electronegativity of the anion.

More detailed discussions of the origin and qualitative interpretation of chemical shifts can be found elsewhere (see BIBLIOGRAPHY). In practice, the interpretation of photoelectron binding energies is based upon tabulated values of chemical shifts (and Auger parameters) that have been measured in specific compounds [see B6]; Table 1 is an example. Alternatively, specific standards – or a range of compounds – can be prepared and/or analyzed for reference.

One must recognize that although *in theory* the binding energy of an electron must reflect any change in its local chemical environment, the associated chemical shift may or may not be observed. In some cases, the shift is too small to be detected because of limited resolution in the measurement. Sometimes, an increase in the instrument resolution can be of benefit, but in many instances, the shift in core level states is not significant. In other cases, effects of relaxation can offset the binding energy shift; e.g., changes in the binding energy due to bond electronegativity may cause corresponding changes in E_R (see equation 2). In the specific case of glass, some important chemical shifts that cannot be detected in routine XPS analyses include Ag^+ vs Ag, Sn^{+2} vs Sn^{+4} and O^{-2} vs OH. Another unfortunate limitation in glass research concerns the measurement of transition metal and rare-earth ion oxidation equilibria. Although the associated shifts in many variable-valence oxides are significant [2.23], their low concentration in most glasses limits detection.

Nevertheless, XPS has proven to be exceedingly beneficial for studying the chemical structure of glass; specifically, non-bridging oxygens in silicate, aluminosilicate and phosphate glasses, bonding in fluoride and chalcogenide glasses, nitridation of oxide glasses, and redox equilibria in glass. And in many of these studies, it has been the bulk chemical structure that has been studied. In these cases, it has been assumed that a clean, vacuum fractured glass creates a surface that exposes the bulk structure of the glass. The uncertainty in this approach concerns the fact that clean surfaces often reconstruct in vacuum [11], and so, the surface is not an ideal projection of the bulk structure. On the other hand, it has been observed that there is reasonable agreement between the measured NBO

concentration and the bulk composition of simple glasses. This agreement could be due to the limited sensitivity of XPS to the outermost monolayer where the reconstruction is confined. In spite of these uncertainties, XPS *is* sensitive to the network chemical structure of a glass – especially BO and NBO – and is necessarily an important tool for the study of these characteristics.

SURFACE SENSITIVITY

The sampling depth in XPS is determined by the *inelastic mean free path* (imfp) of the photoelectrons. This number, often called the *escape depth*, represents the most probable distance the electron can travel in the solid without an energy loss. Any photoelectron or Auger electron that suffers an energy loss before it escapes the solid surface no longer possesses its characteristic energy, and thereby, contributes only to the background signal at an energy, E, which is less than its original energy, E_{ki}. This is reason for the steps in the background at E_{ki} in Figure 2. More precisely, the imfp (λ) characterizes the degree of attenuation of electrons due to inelastic scattering in a homogeneous layer or surface film of thickness x; i.e.,

$$\frac{I_2}{I_1} = e^{-x/\lambda} \tag{9}$$

Thus, photoelectrons that originate more than a distance λ from the surface have less than a 63% chance of escape without experiencing an inelastic scattering event. Another way to think of λ is to recognize that it represents the depth over which 63% of each photoelectron signal originates. A reasonable representation of the *sampling depth of analysis* would be 3λ, where 95% of the detected signal originates.

The imfp of an electron is a function of its kinetic energy, and of the matrix in which it travels. The spectrum in Figure 2 shows the typical range of electron kinetic energy; i.e., 100-1000 eV. In this range, the imfp is of the order .5-5 nm in oxides. The range of imfp is greater in organics (up to 10 nm), and less in metals (.5-3 nm).

It is important to recognize that each peak in the spectrum is due to electrons of different kinetic energy. Thus, the imfp of O1s in Figure 2 is ~2.0 nm, while for Si2p it is ~4.0 nm. This represents a difference in the sampling volume for O and Si It is also important to note that equation 9 is valid only for a homogeneous surface. If the surface is covered with adsorbates or thin layers ($x<\lambda$), the expression must be modified to account for the non-uniformity; that is, the dependence of λ upon the substrate material and the surface film/adsorbate material. These issues are of critical nature in any quantitative analysis, and will be discussed further in the next section.

COMPOSITIONAL ANALYSIS

XPS is probably the most suitable method to measure the surface composition of glass. XPS is less susceptible to charging problems than most of the other surface analysis techniques, it does not introduce any beam damage, and quantitative analysis of the photoelectron spectra is reasonably straightforward.

Equations 10 and 11 define the intensity of the detected photoelectron signal for a specific photoemission line, n, in element i,

$$dI_{i,n} = I_o G \int_{x=0}^{x=\infty} \sigma_{i,n} N_i e^{-x/\lambda} dx \quad (10)$$

$$I_{i,n} = I_o \sigma_{i,n} \lambda_{i,n} N_i G \quad (11)$$

where I_o is the incident x-ray flux, $\sigma_{i,n}$ is the cross-section for photoionization of level n in element i by an x-ray of energy $h\upsilon$, $\lambda_{i,n}$ is the imfp for the emitted photoelectron (which is a function of its kinetic energy and the matrix), N_i is the fraction of atoms i in the sampling volume, and G is an instrumental parameter that accounts for the area of irradiation, the solid angle of the detector, and the transmission of the spectrometer. Equation 11 assumes that the composition of the specimen surface is uniform and homogeneous over the effective sampling volume.

The most common procedure for routine quantitative analysis is through the use of elemental sensitivity factors, S_i. These factors are obtained by measuring I_i for a pure element of i. Since N_i is unity in this case, the measurement gives

$$S_{i,n} = I_o \sigma_{i,n} \lambda_{i,n} G \quad (12)$$

These factors can then be used in the analysis of unknown species; e.g., to determine the ratio of two elements i and j in the surface of a specimen

$$\frac{N_i}{N_j} = \frac{I_{i,n}/S_{i,n}}{I_{j,n}/S_{j,n}} \quad , \quad (13)$$

or the atomic concentration

$$N_i = \frac{I_{i,n}S_{i,n}}{\sum_{\text{all elements } i,j,k\ldots} I_{i,n}/S_{i,n}} \quad (14)$$

The use of the published elemental sensitivity factors [B6] is reasonably accurate in routine XPS analysis of glass surfaces; but the preferred method is to obtain these factors through the use of oxide or compound standards. Figure 7 shows a calibration curve for the N1s signal in various nitride standards. The standards were a series of oxynitride glasses (whose nitrogen contents were determined independently through spectrochemical analysis), and both Si_2N_2O and Si_3N_4 crystals. The ratioing of the N1s intensity provides an internal reference. The slope of this line provides a sensitivity factor that can be used for quantitative surface analysis of N in nitrided glass surfaces or thin films [2.20]. In principal, a calibration curve of the type shown in Figure 7 can be obtained for any species provided that the standards are available, and further, that clean surfaces can be prepared (e.g., by fracture of the glasses in vacuum). The advantage of this procedure over the use of elemental sensitivity factors is that the matrix dependence of the impf is included. In general, the imfp of photoelectrons in oxide glass matrices are greater than those in the pure elements.

The compositions calculated according to equation 11 -- regardless of the method used to obtain the sensitivity factors – assume a homogeneous mixture of the detected elements in the sampling volume of the surface. The thickness of this 'homogeneous layer' is defined by the inelastic mean free path of the photoelectrons used to calculate the composition. In most glasses, this range corresponds to about 4 or 5 nm. This procedure for the quantitative analysis of XPS data is routinely employed, even though it is unlikely that a homogeneous surface layer exists. Most real surfaces – especially glasses – exhibit a strong photoelectron signal due to the presence of (hydro)carbon surface contamination. It is important that this be considered in the interpretation of these analyses.

It is common in many analyses to simply 'ignore' the detected carbon signal and calculate the glass composition using the signals for the 'glass species' only. This approach will give a reasonable measure of the glass composition <u>if</u>: (i) the carbonaceous overlayer itself is uniform and homogeneous, (ii) it does not contain any of the species present in the glass, and (iii) the attenuation of the various substrate signals are equivalent in this layer. In most real glass surfaces, these conditions are very unlikely. The carbonaceous layer most certainly contains oxygen, and the inelastic mean free paths for the various photoelectrons (in the overlayer) may differ by up to 30%.

To demonstrate these points, consider the following experiment. A glass rod of known composition is fractured in <u>air</u> where a layer of carbonaceous contamination forms. It is then subjected to a quantitative XPS analysis. The data in Table 2 summarizes the results. In this case, the true glass surface composition is the bulk composition because the surface was created by fracture. The composition calculated including carbon has implicitly assumed that the carbon is mixed homogeneously within the sampled volume of the glass surface. Obviously, this is not correct in the case of these fracture surfaces. The calculation performed by excluding the carbon signal does not eliminate the error because the carbonaceous overlayer has non-uniformly attenuated the various photoelectrons ejected from the underlying glass substrate. Another source of the error exhibited in Table 2 is due

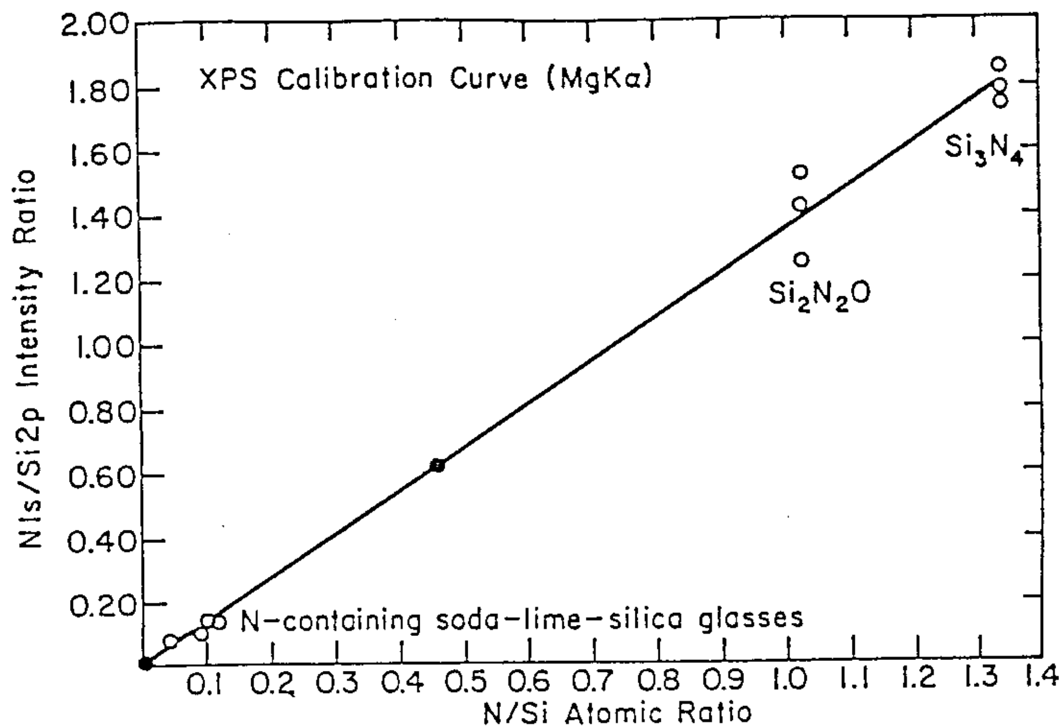

Figure 7. The calibration curve for quantitative analysis of the Nls/Si2p intensity ratio; the N/Si concentration ratios in the glass standards were measured spectrochemically..

Table 2. Glass Surface Compositions in Atomic Percent.

	C	O	Si	Ca	Al	B
measured composition including carbon	8.9	65.0	13.1	6.1	4.1	2.8
measured composition excluding carbon	-	71.3	14.4	6.7	4.5	3.1
true glass surface composition	-	62.2	19.7	8.7	5.8	3.6

to the fact that the carbonaceous layer contains some oxygen. Thus, the oxygen content is overestimated and the metal-ion contents are underestimated in all cases. This problem concerning the interpretation of glass surface composition has no easy solution. In many studies, sputter-etching of the surface is used to remove the layer of carbon. This is not considered an acceptable approach, though, because sputtering can drastically alter the composition of glass surfaces due to differential sputtering and beam-induced migration [12]. It is strongly recommended that compositional analyses be performed in the absence of any ion-beam sputtering. This necessarily means that the problems asociated with the presence of carbon be recognized and considered in the data treatment and interpretation.

There are situations where it is possible to make specific assumptions about the nature of the carbonaceous surface, and quantitatively treat the data accordingly. If a uniform overlayer of carbonaceous contamination is assumed, equation 11 can be modified, so that

$$I'_i = I^0_i e^{-t/\lambda} \tag{15}$$

where t is the thickness of the overlayer, λ is the imfp of the photoelectrons through the carbonaceous overlayer, and I^0_i is the intensity of the photoelectrons in the absence of the overlayer (t=0). One can also write

$$I'_c = I^\infty_c (1 - e^{-t/\lambda}), \tag{16}$$

where I^∞_c is the intensity of the C 1s photoelectron in an infinitely thick layer ($t \gg \lambda$) of carbonaceous contamination. I^0_i can be obtained using a clean vacuum fracture surface or by extrapolation of a set of data for glasses with overlayers of varying thickness. I^∞_i can also be obtained by extrapolation, but for a direct measurement, a pure carbon, hydrocarbon or other 'overlayer' reference standard must be chosen to represent the contamination. The use of this overlayer model is exceedingly useful in those cases where it is known, a priori, that an overlayer exists – e.g., in the study of organic adsorbates on glass surfaces – and where a useful reference standard for the overlayer can be prepared.

But in many cases, a discrete overlayer may not be present on real glass surfaces. The melt-formed surfaces of glass (e.g., fibers, bottles, tubing, etc.) may react with CO_2, H_2O, or hydrocarbons at elevated temperatures where their diffusion into the glass structure is possible. In the polishing and chemical treatment of glass surfaces, carbonaceous overlayers containing constituents of the glass are possible. And in a broader sense, glasses always weather in the ambient atmosphere to form hydrated surface layers that contain carbonates. The point is that it is necessary to establish a model of the glass surface to properly interpret the data. The model usually entails some assumptions about the carbonaceous (or other) overlayer or about the glass substrate composition. Moreover, it often requires calibration of the signals using independent measurements of 'overlayer' standards and/or clean glass fracture surfaces. If the XPS measurements can be made as a function of the angle between the specimen and the detector, the overlayer can be better characterized. This variable angle measurement can be quite useful, but it requires flat, smooth samples to be most effective [see B5].

INSTRUMENTATION

A detailed discussion of the instrumentation used in XPS will not be provided here because many other sources are available [see BIBLIOGRAPHY]. Only a commentary will be provided about the important features and specialized facilities for glass research. The basic apparatus is represented in Figure 1. An ultra high vacuum system, an x-ray source, an electron energy analyzer and a computerized data acquisition system. Some auxilliary items that may be of benefit include an ion sputtering gun, a fracture stage, a variable-angle specimen holder, an electron flood gun, and a metal evaporation source.

The vacuum system, and especially the availability of a fracture stage, are important in glass research because it is common to use XPS – an inherently surface sensitive technique – for bulk characterization. This necessitates an atomically clean surface that is best obtained by fracturing glass rods in vacuum. Clean fracture surfaces can also be used as calibration standards for quantitative surface analysis. A vacuum level better than 10^{-8} Pa is required to maintain the fracture surface in a clean state.

In most commercial XPS systems, MgKα and AlKα x-ray sources are standard. Although the routine analysis of most materials, including glass, can be achieved with these soft x-rays, there are a couple of specific applications in glass where higher energy x-rays, and monochromatic x-ray sources, can be advantageous. A higher energy x-ray source – e.g., SiKα, TiKα or ZrLα – creates core holes that lead to additional Auger lines in the XPS spectrum. These Auger lines can be used to obtain Auger parameters that are useful for structural characterization of silicates and for calibration of charging effects. The use of a monochromatic x-ray source improves the resolution of the analysis and this can be of benefit in the measurement of small chemical shifts. This is because the ability to measure small differences in binding energy, ΔE_b, depends upon the linewidth of the incident x-ray, $\Delta(h\upsilon)$ (see equation 1).

APPLICATIONS OF XPS

Non-Bridging Oxygens

This example illustrates a bulk analysis of the network chemical structure, specifically non-bridging oxygens, in silicate glasses. Since the bulk structure was of interest, clean surfaces created by (vacuum) fracture were required.

Figure 8 shows high resolution O1s spectra for sodium aluminosilicate glasses with various Al/Na ratios. The relative concentration of bridging oxygen (BO) and non-bridging oxygen (NBO) is readily obtained through deconvolution; the presence of a distinct line due to the NBO is obvious. The ratio of the integrated intensities is equal to the concentration ratio because the sensitivity factors for the oxygen states are virtually identical. This analysis shows that the addition of Al_2O_3 eliminates NBO in sodium-silicate glasses. In this study, though, two different bridging oxygen sites were proposed – one due to Si-O-Si (BO1) and the other due to Si-O-Al (BO2) – even though these two BO lines are not resolved in the raw data [2.17]. A higher resolution measurement could provide more direct evidence of the authors' interpretation of the data. In the absence of experimental evidence of two distinct BO lines, they have based their interpretation of the data upon a specific model of the glass structure, and a systematic broadening and shifting of the proposed (BO1 + BO2) components. In general, curve fitting and deconvolution of XPS peaks should be executed with caution.

Figure 9 shows the high-resolution O1s spectra for binary alkali-silicate glasses containing Li, Na, K or Cs. The fact that the ratio of the BO to NBO lines is nearly equal in each glass is consistent with the fact that the glass specimens were of equal molar composition. However, it can be seen that the binding energy of the (NB)O1s electron depends upon the specific alkali specie in the glass.This reveals the dependence of the (NB)O1s binding energy upon the field strength of the associated alkali. This clearly demonstrates the sensitivity of the NBO photoelectron binding energy to its specific environment.

The interested reader can find many other studies of BO and NBO in binary and ternary silicate and phosphate glasses [see 2]. In more complex multicomponent glasses, where a wider distribution of oxygen sites exists, it is more difficult to resolve the BO and NBO lines. Only a broadening and/or a gradual shift of the O1s line is observed [2.33]. The ability to resolve distinct binding energy states for BO and NBO seems to be unique to simple binary or ternary oxides. Similarly, there have been attempts to measure non-bridging fluorine in fluoride glasses, but only a broadening of the F1s line has been reported [2.18].

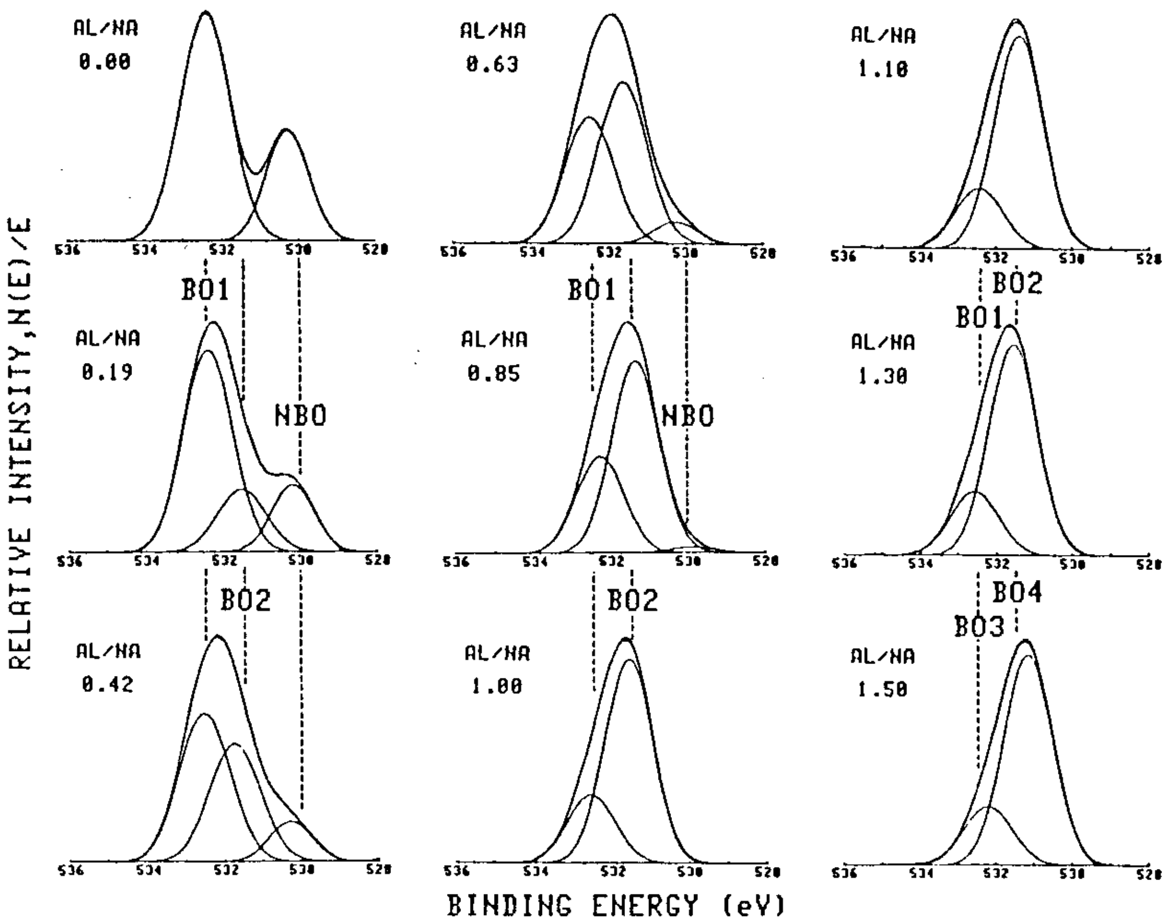

Figure 8. The high-resolution Ols spectra for sodium-aluminosilicate glasses with various Al/Na concentration ratios; each spectra was deconvoluted assuming three Gaussian components of constant width but varying binding energy [from 2.17].

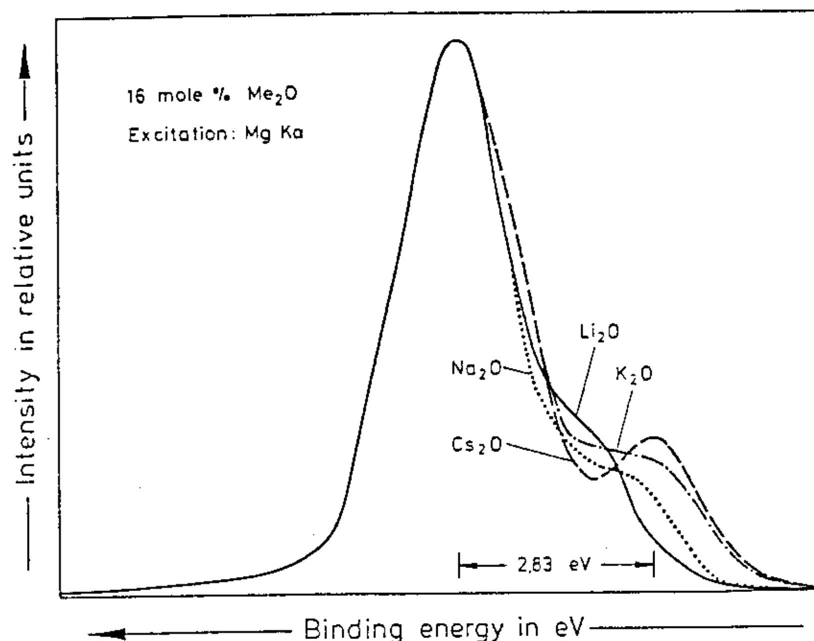

Figure 9. High-resolution Ols spectra of alkali silicate glasses with 16 mol-% Me_2O where Me = Li, Na, K or Cs [from 2.3].

Thermochemical Treatment of Glass Surfaces

This example demonstrates the ability to characterize changes in the surface structure and redox state of a glass surface [2.28]. Figure 10 shows the high resolution O1s spectra of two alkali-lead-silicate glass specimens. One is for a vacuum fracture surface, and represents the bulk structure. The presence of two different oxygen species is clearly evident, and presumably, these correspond to BO and NBO. After a surface treatment in hydrogen, elimination of the lower binding energy O1s is observed. Figure 11 shows the high-resolution Pb4f spectra of these specimens. It is most evident that the Pb concentration has been significantly lowered in the treated surface. This probably accounts for the elimination of NBO. After low-energy ion sputtering into the sub-surface of the treated glass, the Pb concentration increases, but it can be seen that the oxidation state of the Pb has been altered. The Pb4f lines have shifted to lower binding energy. Using reference spectra for the identification, it was concluded that these were metallic Pb species. Thus, the hydrogen treatment (at ~500°C) converted the PbO to Pb, and evaporation of Pb at the surface created a silica-rich zone. The

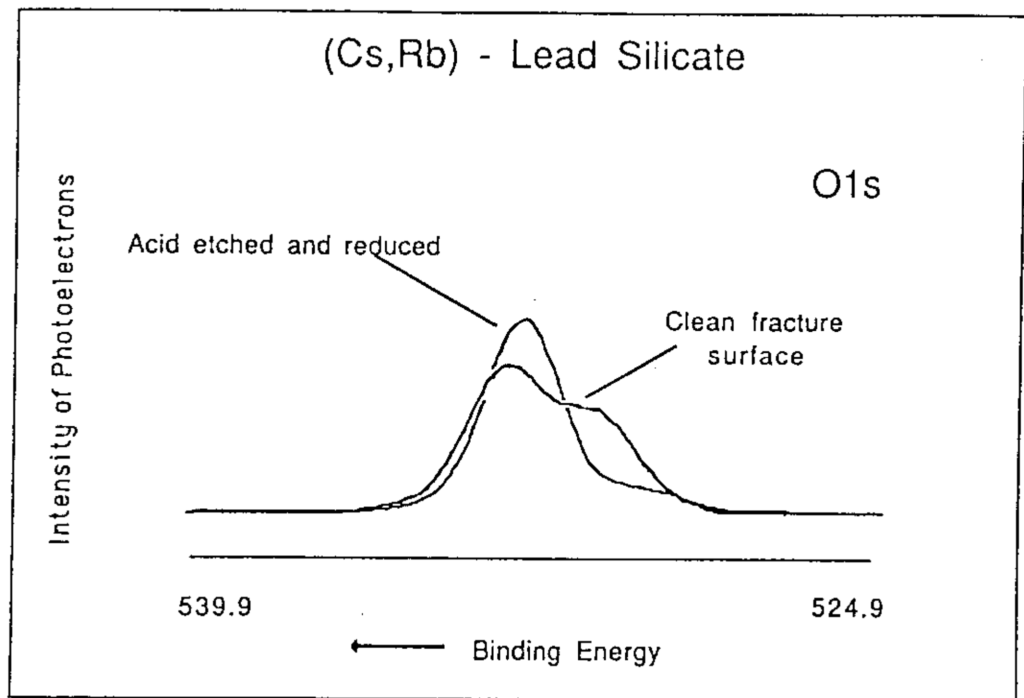

Figure 10. High-resolution Ols spectra of an alkali-lead-silicate glass before and after hydrogen reduction at 485°C.

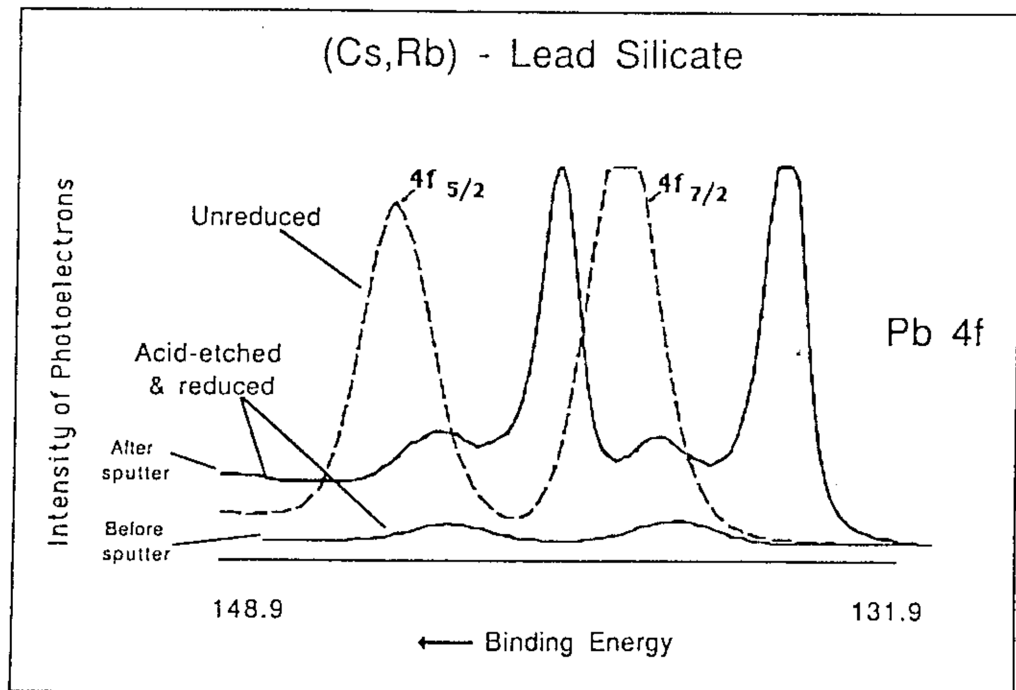

Figure 11. High-resolution Pb4f spectra of an alkali-lead-silicate glass before and after hydrogen reduction at 485°C.

reader should note that, in general, ion sputtering must be used with caution because it can change the composition and chemistry of the surface being analyzed [12]. In this analysis, ion sputtering of the clean fracture surface verified the absence of any perturbing effects of the ion bombardment at low energy.

Chemical and Compositional Analysis of Sol/Gel Thin Films

This example demonstrates the ability of XPS to provide *quantitative* chemical and compositional analysis of glasses – in this case glass thin films [13]. It also shows that with careful calibration, the binding energy value itself can provide a measure of composition. In this way, a quantitative composition determination can be obtained which is independent of the usual integrated intensity analysis.

Figure 12 shows the high resolution C1s spectra of silica sol/gel films after various heat treatments; the spectra of thermal SiO_2 is also shown for reference. The thermal SiO_2 exhibits only 'adventitious' carbon due to contamination in the atmosphere, whereas the SiO_2 sol/gel films show other chemical states of carbon due to their processing history. These lines were identified using published reference spectra [B6].

Figure 7 showed the calibration curve established for quantitative analysis of nitrogen in the ammonia treated silica films. It was used to determine the nitrogen concentration in films treated at various temperatures. These nitrogen concentrations were then plotted against the Si2p binding energies; this plot is shown in Figure 13. The data reveals that the progressive incorporation of nitrogen influences the Si2p binding energy, and thereby, provides evidence for chemical association of the Si and N in the treated films. The fact that the Si2p binding energy in Si_2N_2O is ~ 102 eV provides strong evidence for the creation of Si-oxynitride species in the nitrided silica gel-film. (A theoretical discussion of this binding energy effect can be found in 2.20.) Figure 13 also provides an additional calibration curve for nitrogen concentration based solely on the Si2p binding energy.

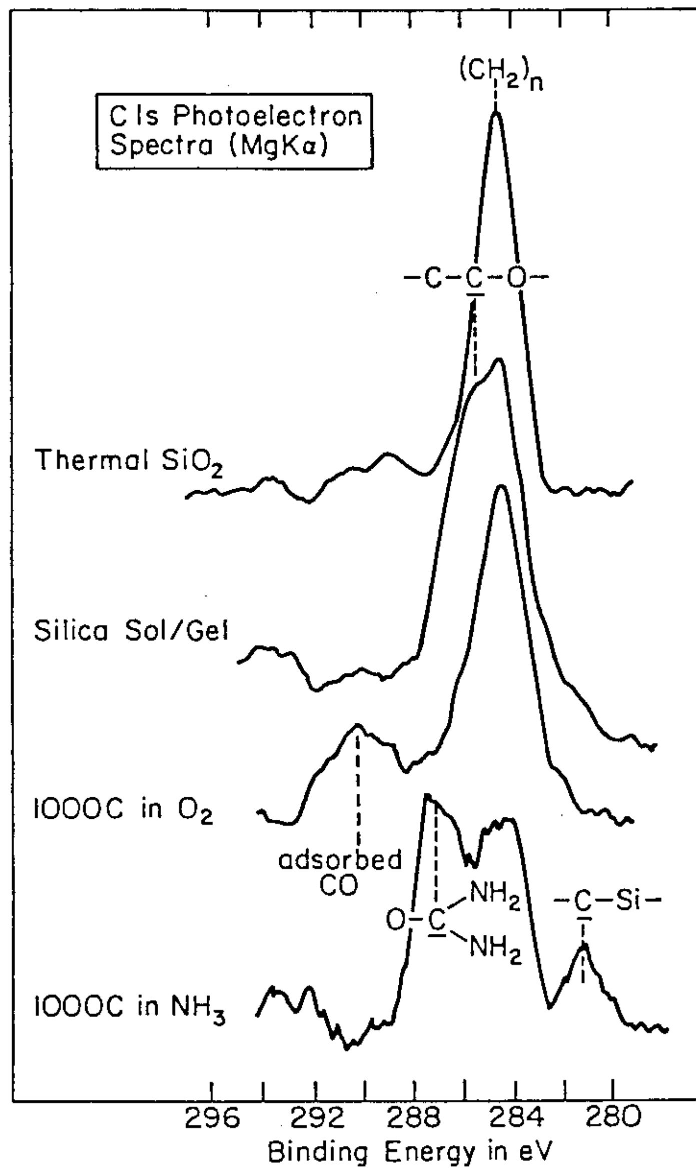

Figure 12. High resolution Cls spectra of an SiO_2 reference standard and SiO_2 sol/gel thin film before and after thermal processing.

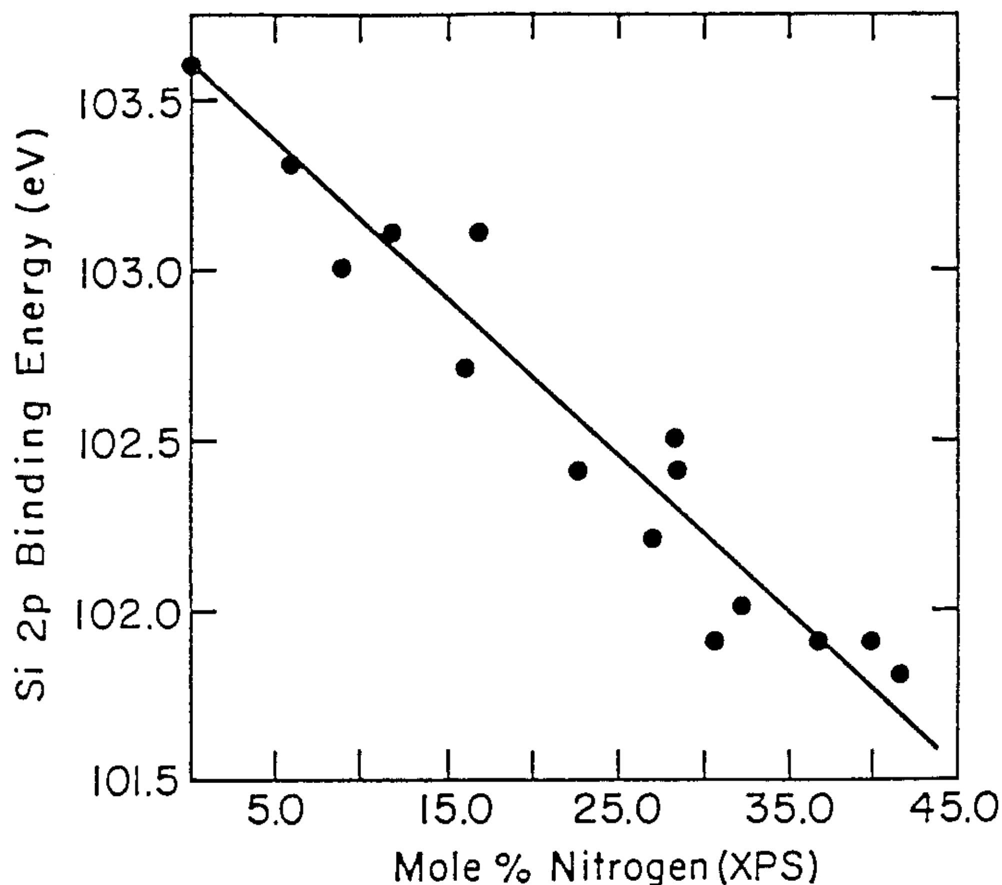

Figure 13. The observed relationship between the Si2p binding energy and nitrogen content of silica sol/gel films treated in ammonia at various temperatures.

Organic Adsorbates on Glass

XPS is very useful for the detection and chemical analysis of organics on glass surfaces. In comparison to electron-beam and ion-beam methods, the x-ray beam is relatively non-destructive. Moreover, the photoelectron spectra can distinguish the chemical state of the organic species. In this example, glass fibers were analyzed after exposure to five different organic silanes. Untreated fibers were examined for reference. The spectra were quantitatively evaluated using elemental sensitivity factors. A calculation of the fiber surface composition according to equation 14 revealed that all of the treated fibers had considerably more carbon on the surfaces (30-50 a/o) than the untreated control fibers (10-15 a/o). Naturally, this is due to

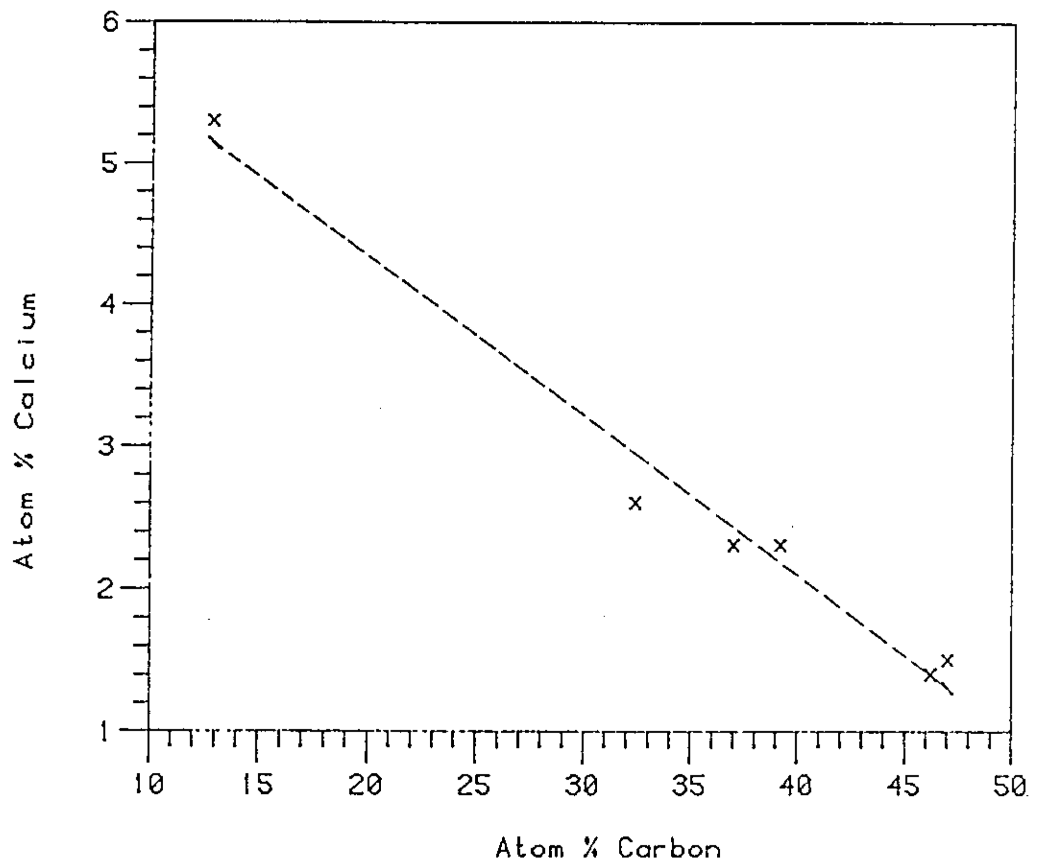

Figure 14. The observed relationship between the calculated Ca and C concentrations (or equivalently, the relative Ca2p and Cls signals) on E-glass fibers treated with organic silanes..

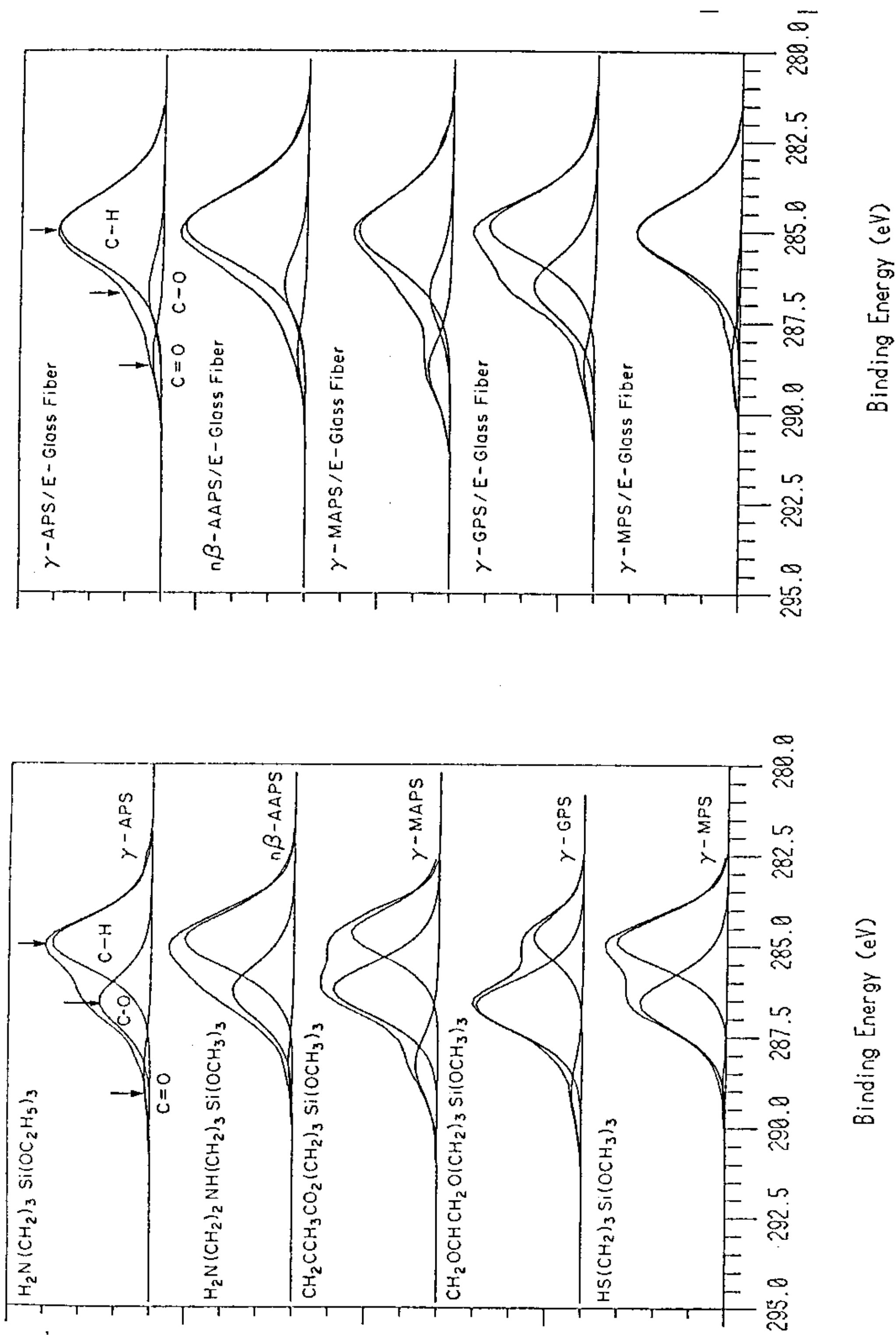

Figure 15. High resolution Cls spectra of organosilanes neat on gold foil (left) and adsorbed to E-glass fibers (right).

adsorption of the organic silanes, and for qualitative characterization, these analyses could be sufficient to show the relative effects of the silane-treatment.

Figure 14 plots the carbon concentrations against the calcium concentrations. The fact that the Ca concentration (associated with the glass fiber) decreases with increasing C concentration verifies that the carbon is associated with an overlayer. But clearly, the *Ca concentrations* are quantitatively meaningless unless they are interpreted using a more representative model of the surface; i.e., the analyzed surface is not a homogeneous mixture of the organic silane and glass. The data in Figure 13 is, in fact, plotted according to Equations 15 and 16. An extrapolation of the line to 0% carbon – that is, no overlayer @ t=0 – gives a value of 6.5% Ca at the glass fiber surface. This is in reasonable agreement with the glass composition (~7.5% Ca). And, the slope of this line allows the thickness of the overlayers to be determined. Assuming a value of $\lambda \approx 2.7$ nm, the overlayers are found to be 1.5-2.5 nm. These thicknesses correlated with the length of the alkyl group in the various silanes [2.30].

In this analysis, it was also possible to examine the chemistry of the adsorbed silane, and compare it to the bulk silane, using the high-resolution C1s spectra. Figures 15a and 15b compares these spectra for all five the silanes. The spectra were deconvoluted to separate C=O, C-O and C-H sites in the silane. The relative decrease in the C-O species in the *adsorbed* silane verifies that hydrolysis of the alkoxy ligands in the silane has occurred.

SUMMARY

The most common applications of XPS in glass research involve surface analysis; that is, the determination of surface composition and/or the identification of surface impurities or adsorbates. The technique is especially suited to the analysis of organic and metallic species on the surface, although a reasonable quantitative analysis of the glass composition itself can also be achieved. The analysis is limited to species located in the outermost 0.5-5.0 nm of surface whose concentration exceeds .1-1 atomic percent. It should be noted, though, that XPS cannot detect hydrogen. XPS can also be used to characterize features of the chemical structure; that is, non-bridging oxygens, bonding or oxidation state of anions and cations, and valence band density of states. And is those cases where very clean fracture surfaces can be prepared, the spectra can be used to characterize the bulk chemical structure of the glass.

ACKNOWLEDGEMENTS

The author thanks his colleagues and students for their contributions toward this review: Dick Brow, Lee Carman, Fumio Ohuchi, Bill Tasker, Alan Then and Tom Wittberg.

BIBLIOGRAPHY

B1. K. Siegbahn, C. N. Nordling, A. Fahlman, R. Nordberg, K. Hamrin, J. Hedman, G. Johansson, T. Bergmark, S. E. Karlsson, I. Lindgren, and B. Lindberg, *ESCA, Atomic, Molecular, and Solid State Structure Studied by Means of Electron Spectroscopy* (Almqvist and Wiksells, Uppsala, Sweden, 1967).

B2. T. A. Carlson, *Photoelectron and Auger Spectroscopy* (Plenum Press, New York, 1975).

B3. P. K. Ghosh, *Introduction to Photoelectron Spectroscopy* (Wiley-Interscience Publishers, New York, 1983).

B4. C. R. Brundle and A. D. Baker, Eds., *Electron Spectroscopy: Theory, Techniques and Applications*, Vol. 1-5 (Academic Press, London, 1978).

B5. D. Briggs and M. P. Seah, *Practical Surface Analysis by Auger and X-ray Photoelectron Spectroscopy* (John Wiley and Sons, New York, 1983).

B6. D. Briggs, Ed., *Handbook of X-ray and Ultraviolet Photoelectron Spectroscopy* (Heydon and Son, London, 1977, 1978).

REFERENCES

1. See for example:
1.1. D. A. Stephenson and N. J. Binkowski, "X-ray Photoelectron Spectroscopy of Silica in Theory and Experiment," J. Non-Cryst. Solids, 22[2], 399-421 (1976).
1.2. S. R. Nagel, J. Tauc, and B. G. Bagley, "X-ray Photoemission Study of a Soda-Lime-Silica Glass," Solid State Commun., 20[3], 245-9 (1976).
1.3. B. Fischer, R. A. Pollak, T. H. DiStefano, and W. D. Grobman, "Electronic Structure of SiO_2, $Si_xGe_{1-x}O_2$, and GeO_2 from Photoemission Spectroscopy," Phys. Rev., B15[6], 3193-9 (1977).
1.4. W. Y. Ching, R. A. Murray, D. J. Lam, and B. W. Veal, "Comparative Studies of Electronic Structures of Sodium Metasilicate and α and β Phases of Sodium Disilicate," Phys. Rev., B28[8], 4724-34 (1983).
1.5. W. Y. Ching, Y. P. Li, B. W. Veal, and D. J. Lam, "Electronic Structures of Lithium Metasilicate and Lithium Disilicate," Phys. Rev., B32[2], 1203-7 (1985).
2. See for example:
2.1. J. H. Escard and D. J. Brion, "Study of Composition of Leached Glass Surfaces by Photoelectron Spectroscopy," J. Am. Ceram. Soc., 58[7-8], 296-299 (1975).
2.2. N. J. Binkowski, R. F. Heitzenrater, and D. A. Stephenson, "Surface Analysis of a Treated Soda-Lime Glass," J. Am. Ceram. Soc., 59[3-4], 153-7 (1976).

2.3. R. Bruckner, H.-U. Chun, and H. Goretzki, "Photoelectron Spectroscopy (ESCA) on Alkali Silicate and Soda Aluminosilicate Glasses," Glastechn. Ber., 51[1], 1-7 (1978).
2.4. Y. Kaneko, "Application of Photoelectron Spectroscopy to Glasses," Yogyo-Kyokai-Shi, 86[7], 330-3 (1978).
2.5. R. Gresh, W. Müller-Warnuth, and H. Dutz, "X-ray Photoelectron Spectroscopy of Sodium Phosphate Glasses," J. Non-Cryst. Solids, 34, 127-136 (1979).
2.6. J. S. Jen and M. R. Kalinowski, "An ESCA Study of the Bridging to Non-Bridging Oxygen Ratio in Sodium Silicate Glass and the Correlations to Glass Density and Refractive Index,", J. Non-Cryst. Solids, 38-39, 21-6 (1980).
2.7. D. J. Lam, A. P. Paulikas, and B. W. Veal, "X-ray Photoemission Spectroscopy Studies of Soda Aluminosilicate Glasses," J. Non-Cryst. Solids, 42[1-3], 41-8 (1980).
2.8. R. Bruckner, H.-U. Chun, H. Goretski, and M. Sammet, "XPS Measurements and Structural Aspects of Silicate and Phosphate Glasses," J. Non-Cryst. Solids, 42[1-3], 49-60 (1980).
2.9. B.M.J. Smets and T.P.A. Lommen, "The Structure of Germanosilicate Glasses, Studied by X-ray Photoelectron Spectroscopy," J. Non-Cryst. Solids, 46[1], 21-32 (1981).
2.10. B.M.J. Smets and T.P.A. Lommen, "The Incorporation of Aluminum Oxide and Boron Oxide in Sodium Silicate Glasses, Studied by X-ray Photoelectron Spectroscopy," Phys. Chem. Glasses, 22[6], 158-62 (1981).
2.11. T. Sasaki, M. Kawaguchi, M. Yamane, and Y. Suginohara, "On the Quantitative Analysis of O°, O^{-}, and O^{2-} Ions in Binary Silicate by X-ray Photoelectron Spectroscopy," J. Japan Inst. Metals, 45[8], 790-6 (1981).
2.12. K. Matsumoto, "The Analysis of Carbon on the Surface of Glass by ESCA," Yogyo-Kyokai-Shi," 89[1], 19-23 (1981).
2.13. B. W. Veal, D. J. Lam, A. P. Paulikas, and W. Y. Ching, "XPS Study of CaO in Sodium Silicate Glasses," J. Non-Cryst. Solids, 49[1-3], 309-20 (1982).
2.14. Y. Kaneko, H. Nakamura, M. Yamane, K. Mizoguchi, and Y. Suginohara, "Photoelectron Spectra of Silicate Glasses Containing Trivalent Cations," Yogyo-Kyokai-Shi, 91[7], 321-4 (1983).
2.15. R. K. Brow and C. G. Pantano, "Nitrogen Coordination in Oxynitride Glasses," J. Am. Ceram. Soc., 67[4], C72-74 (1984).
2.16. M. Sekita, A. Fujimori, A. Makishima, T. Shimohira, and H. Ohashi, "X-ray Photoelectron Spectroscopy of a Caerium-Doped Lanthanum Aluminosilicate Glass," J. Non-Cryst. Solids, 76, 399-407 (1985).
2.17. G. W. Tasker, D. R. Uhlmann, P.I.K. Onorato, M. N. Alexander, and C. W. Struck, "Structure of Sodium Aluminosilicate Glasses: X-ray Photoelectron Spectroscopy," J. DePhysique, C8[46], C8-273-80 (1985).
2.18. R. M. Almeida, J. Lau, and J. D. Mackenzie, "XPS Studies of Fluorozirconates," Mat. Sci. Forum, 6, 465-470 (1985).
2.19. D. S. Goldman, "Evaluation of the Ratios of Bridging to Nonbridging Oxygens in Simple Silicate Glasses by Electron Spectroscopy for Chemical Analysis," Physics and Chemistry of Glasses, 27[3], 128-133 (1986).

2.20. R. K. Brow and C. G. Pantano, "Compositionally Dependent Si 2p Binding Energy Shifts in Silicon Oxynitride Thin films," J. Am. Ceram. Soc., 69[4], 314-16 (1986).
2.21. G. W. Tasker, "X-ray Photoelectron Spectroscopy of Silicate Glasses," Ph.D. Thesis, Massachusetts Inst. of Tech., 1987.
2.22. R. K. Brow, "Oxidation States of Chromium Dissolved in Glass Determined by X-ray Photoelectron Spectroscopy," J. Am. Ceram. Soc., 70[6], C-129-31 (1987).
2.23. B. W. Veal, J. N. Mundy and D. J. Lam, "Actinides in Silicate Glasses," *Handbook on the Physics and Chemistry of the Actinides*, A. J. Freeman and G. H. Lander, Eds. (Elsevier, 271-309, 1987).
2.24. C. G. Pantano and R. K. Brow, "Hydrolysis Reactions at the Surface of Fluorozirconate Glass," J. Am. Ceram. Soc., 71[7], 577-81 (1988).
2.25. R. Caracciolo and S. H. Garofalini, "X-ray Photoelectron Spectroscopy Analysis of Potassium Adsorption onto υ-SiO_2: Observation of Reactive Surface Defect Sites," J. Am. Ceram. Soc., 71[7], C346-C349 (1988).
2.26. R. K. Brow, M. R. Reidmeyer and D. E. Day, "Oxygen Bonding in Nitrided Sodium-and Lithium-Metaphosphate Glasses," J. Non-Cryst. Solids, 99, 178-189 (1988).
2.27. R. K. Brow, Y. Zhu, D. E. Day, and G. W. Arnold, "Surface Nitridation of a Phosphate Glass," J. Non-Cryst Solids, 120, 172-7 (1990).
2.28. A. M. Then and C. G. Pantano, "Formation and Behavior of Surface Layers on Electron Emission Glasses," J. Non-Cryst. Solids, 120 178-187 (1990).
2.29. Z. A. Osborne, R. K. Brow, D. R. Tallant, "Short-Range Structure of Fluorine-Modified Phosphate Glass," *Properties and Characteristics of Optical Glass, II*, SPIE Proceedings, 1990 Int. Symp. on Optical and Optoelectronic Apl. Sci. and Eng., San Diego, CA, July 8-13, 1990.
2.30. C. G. Pantano and T. N. Wittberg, "XPS Analysis of Silane Coupling Agents and Silane-treated E-glass Fibers," Surf. and Int. Anal., 15, 498-501 (1990).
2.31. R. K. Brow, R. J. Kirkpatrick, and G. L. Turner, "Local Structure of $xAl_2O_3 \cdot (1-x)NaOP_3$ Glasses: An NMR and XPS Study," J. Am. Ceram. Soc., 73[8], 2293-2300 (1990).
2.32. D. Sprenger, H. Bach, W. Meisel and P. Gütlich, "XPS Study of Leached Glass Surfaces," J. Non-Cryst. Solids, 126, 111-129 (1990).
2.33. I. Berthelot and P. Lehuede, "XPS Analysis of Glass: O1s Line Study," Rivista della Staz. Sper. Vetro, n.6 (1990).
3. P. Swift, "Adventitious Carbon - The Panacea for Energy Referencing?" Surf. Interface Anal., 4[2], 47-51 (1982).
4. S. Hohiki and K. Oki, "Problems of Adventitious Carbon as an Energy Reference," J. Electron Spectrosc. Relat. Phenom., 33[4], 375-80 (1984).
5. C. R. Ginnard and W. M. Riggs, "Gold Evaporation for Charge Correction in X-ray Photoelectron Spectroscopy," Anal. Chem., 46[9], 1306-8 (1974).
6. Y. Uwamino, T. Ishizuka, and H. Yamatera, "Charge Correction by Gold Deposition onto Non-Conducting Samples in X-ray Photoelectron

Spectroscopy," J. Electron Spectrosc. Relat. Phenom., 23[1], 55-62 (1981).

7. S. Kohiki, T. Ohmura, and K. Kusao, "A New Charge-Correction Method in X-ray Photoelectron Spectroscopy," J. Electron Spectrosc. Relat. Phenom., 28[4], 229-37 (1983).
8. S. Kohiki and K. Oki, "An Appraisal of Evaporated Gold as an Energy Reference in X-ray Photoelectron Spectroscopy," J. Electron Spectrosc. Relat. Phenom., 36[1], 105-10 (1985).
9. M. J. Edgell, D. R. Baer, and J. E. Castle, "A Test of Biased Referencing for the XPS Analysis of Nonconducting Materials," J. Vac. Sci. Technol., A4[3], 1562-3 (1986).
10. J. E. Castle and R. H. West, "Bremsstrahlung-Induced Auger Peaks," J. Elect. Spec., 18, 355-358 (1980).
11. C. G. Pantano, "Glass Surfaces," Rev. of Solid State Sci., 3[3&4], 379-408 (1989)
12. C. G. Pantano, "Chemical and Compositional Analysis of Glass Surfaces," Rivista della Staz. Sper. Vetro, n.6, 123 (1991).
13. R. K. Brow and C. G. Pantano, "Thermochemical Nitridation of Microporous Silica Films in Ammonia," J. Am. Ceram. Soc., 70[1], 9-14, 1987.